An RSFQ Variable Duty Cycle Oscillator for Driving a Superconductive Qubit

Donald S. Crankshaw, Jonathan L. Habif, Xingxiang Zhou, Terry P. Orlando, Marc J. Feldman, and Mark F. Bocko

Abstract—We design an RSFQ oscillator with a variable duty cycle to drive a superconductive qubit. This design has been optimized to minimize the decoherence when coupled to the superconductive persistent current qubit. A continuous RSFQ ring oscillator reads the contents of a Non-Destructive Read Out memory cell. By using two out-of-phase counters to Set and Reset the cell, we can vary the duty cycle of the pulses read from the memory cell. This train of flux quanta is filtered, then used to drive the persistent current qubit. The precision is sufficient to measure relaxation time and possibly Rabi oscillations.

Index Terms—Oscillator, quantum computation, qubit, RSFQ.

I. INTRODUCTION

THE recent interest in superconductive technology as the basis for quantum computation has sparked renewed interest in high-speed, on-chip control electronics [1]–[7]. RSFQ forms the basis of an ultrafast, digital logic technology based on superconductive Josephson junctions which can be integrated on-chip with superconductive quantum circuits. In RSFQ technology, a quantum of magnetic flux, stored as a current in a loop, represents the logical 1. These flux quanta can rapidly traverse circuits of Josephson junctions, which serve as buffers to propagate them. Used in combination, Josephson junctions can also cause the flux quanta to interact to perform logic operations.

In this paper, we use a variable duty cycle RSFQ oscillator to drive the persistent current qubit described in [1]. This qubit has the parameters we describe in [8], with $I_c = 1.25$ μA, $E_J/E_C = 350$, and $\alpha = 0.65$. Lincoln laboratory's foundry has produced both the qubit and the RSFQ circuit in a 500 A/cm^2 process [9].

II. THE CIRCUIT DESIGN

Fig. 1 shows the block diagram of the oscillator circuit. The 8 GHz clock (consisting of a JTL ring) serves as an always-on RSFQ oscillator. Its signal is sent to the Read input of the NDRO (Non-Destructive Read Out) memory cell every 125 ps. If there is a 1 in the memory cell, then a pulse is sent to the JTL and

D. S. Crankshaw and T. P. Orlando are with the Electrical Engineering and Computer Science department at the Massachusetts Institute of Technology, Cambridge, MA 02139 USA (e-mail: dscrank@mit.edu).

J. L. Habif, X. Zhou, M. J. Feldman, and M. F. Bocko are with the Electrical and Computer Engineering at the University of Rochester, Rochester, NY 14627 USA (e-mail: habif@ece.rochester.edu).
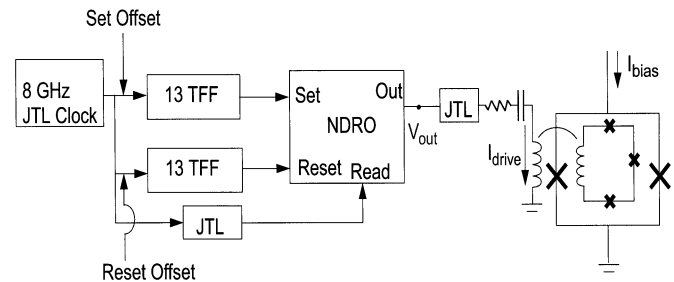
Fig. 1. A block diagram of the variable duty cycle oscillator. Two T-flip-flop counters send their overflow pulses to the Set and Reset inputs of a nondestructive read out memory cell. The phase difference between the counters determines the proportion of the counter period for which the NDRO is on or off. A read signal sent to the NDRO every clock cycle will either read a 1 and cause it to transmit a signal, or a 0 and cause no response. The resulting output is filtered and then delivered to the qubit. This circuit has been fabricated at Lincoln Laboratory's foundry.

is transmitted to the qubit after filtering. If there is a 0 in the memory cell, no pulse is sent. The Set and Reset on the memory cell are controlled by two counters, each of which is made up of a chain of T-flip-flops which increment at each pulse from the 8 GHz clock from 0 to $2^{13} - 1$, or 8191. There are 13 T-flip-flops in each chain because that number gives the counters a period of about 1 μs. When the counter connected to the Set input of the memory cell overflows, turning over from 8191 to 0, it sends the overflow pulse to the Set input of the NDRO to store a 1 in the cell. Likewise, the other counter will reset the NDRO cell when it overflows. We can set the initial states of the two counters to create an offset which determines the on-time of the NDRO cell. If the Set counter fills up 10 pulses before the Reset counter does, the circuit will transmit 10 pulses to the qubit, then stop until the next time the Set counter overflows.

The oscillator may thus be adjusted to transmit anywhere from 1 to 8191 pulses to the qubit every counter period, corresponding to the number of counts by which the two TFF chains are out-of-phase. The fine degree of control available is advantageous for causing controlled oscillations in the qubit. The signal coming out of the NDRO goes through an RLC filter before reaching the qubit, removing some of the harmonics before they cause unwanted transitions and subsequent decoherence. The filter has parameters of $R_c = 1.8$ Ω, $L_c = 68$ pH, and $C_c = 10$ pF, such that the resonant frequency is 6.8 GHz, and the Q is 2.1. Fig. 2(a) shows the pulse train transmitted by the JTL, while (b) shows the filtered signal which couples to the qubit inductively. The qubit sees an oscillating magnetic field corresponding to $M_{mw}I_{\text{drive}}$.
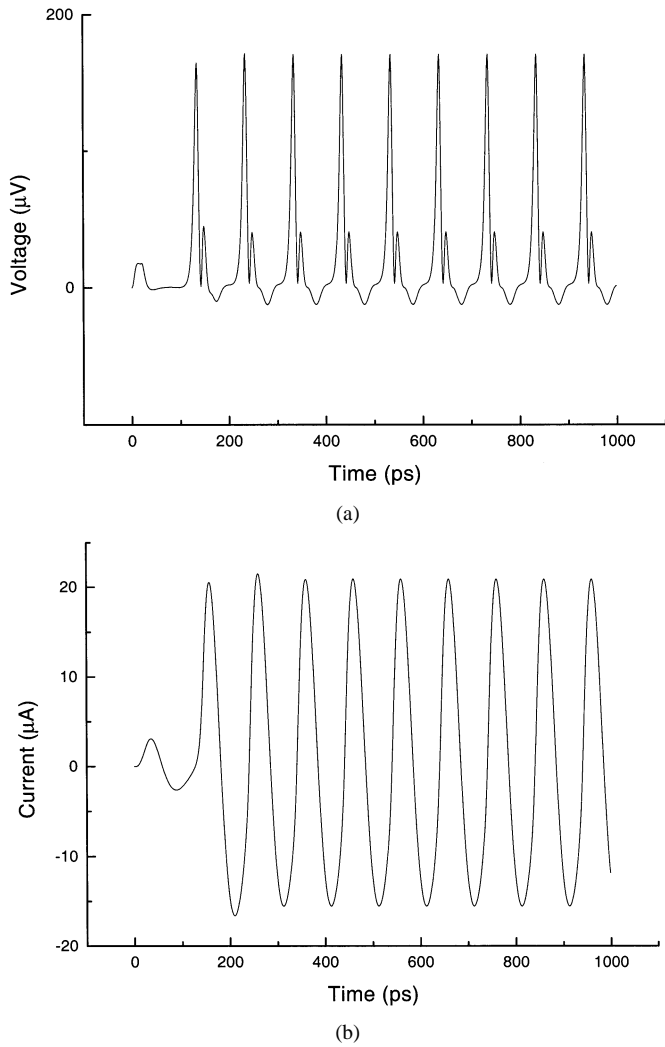
(a)

(b)

Fig. 2. (a) The signal which travels down the JTL. These voltage pulses are clearly nonsinusoidal. (b) Once it passes through an RLC filter, the signal from the NDRO produces a nearly sinusoidal current across the inductor, which translates this signal into the magnetic field which couples to the qubit.
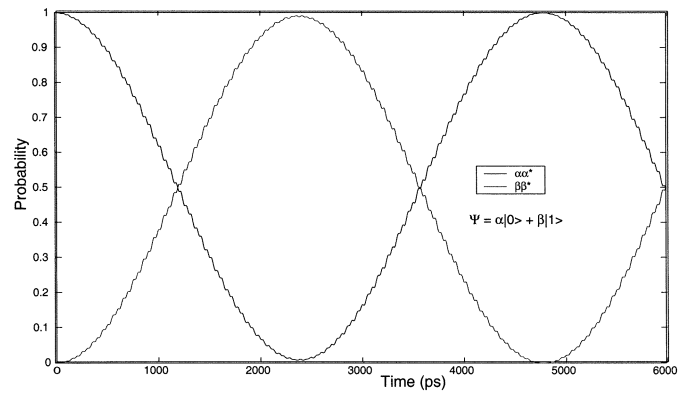

Fig. 3. The population of the qubit's first two energy levels as a function of time in response to driving at the energy splitting. The total wavefunction is $\alpha|0\rangle + \beta|1\rangle$.

III. THE QUBIT

A. Qubit Rotation

This variable duty cycle oscillator is only the first half of the experiment. While it may be useful in any number of superconductive qubit experiments, the design as fabricated is is coupled to the persistent current qubit, and its parameters are chosen minimize decoherence in the qubit system using the methods described in [10].

Applying a microwave source resonant to the energy splitting between the ground state and the first excited state of the qubit will cause Rabi oscillations. A flexible model which can handle an arbitrary waveform and which takes into account the full quantum model of the qubit is used to calculate the oscillations.

The wavefunction of the qubit evolves according to (1)

$$\Psi(t) = \sum_i c_i(0)\psi_i \exp\left(\frac{-iE_i t}{\hbar}\right). \tag{1}$$

In this equation, Ψ is the overall wavefunction, made up by the sum of basis states ψ_i, each of which is the wavefunction associated with energy level E_i. c_i is the coefficient corresponding to the weight and phase of each basis state. When the potential landscape of the qubit changes at time t_0, as happens when the magnetic field biasing the qubit changes, the wavefunction is projected into new basis states, which then evolve according to the new energy levels. To determine the coefficients for each of these new basis states, the total wavefunction, Ψ, is projected onto each of the new basis states, ϕ_i, giving the coefficients $b_i = \langle\phi_i|\Psi\rangle$. The new wavefunction evolves by (2)

$$\Psi(t) = \sum_i b_i\phi_i(t_0) \exp\left(\frac{-iE_i'(t - t_0)}{\hbar}\right). \tag{2}$$

Here, E_i' are the energies associated with the new potential. A continuously varying potential can be discretized to make it compatible with this method.

Although most solid state quantum systems have more than two energy levels, the measurement projects the system into two distinguishable states, which are labeled the $|0\rangle$ and $|1\rangle$ states. These measured states are not necessarily the basis states during the qubit's evolution. Fig. 3 shows a simulation of the population of the $|0\rangle$ and $|1\rangle$ states in a persistent current qubit, biased with a DC magnetic field of $0.497 \, \Phi_0$, when it starts in the $|0\rangle$ state and is then driven by an oscillating magnetic field with the waveform shown in Fig. 2(b), the output of the oscillator described in this paper. The amplitude of the oscillating magnetic field is $\delta\Phi = 0.001 \, \Phi_0$. The $|0\rangle$ and $|1\rangle$ states correspond to the ground and first excited states respectively when the flux bias of the qubit is $0.497 \, \Phi_0$.

B. Decoherence

We used the method in [10] to estimate and minimize the contribution which the RSFQ electronics make to decoherence in the qubit. In this method, the spin-boson model determines the influence of noise on the relaxation and dephasing times, producing in (3) and (4)

$$\frac{1}{\tau_r} = \frac{1}{2}\left(\frac{\Delta}{\nu}\right)^2 J(\omega) \coth\left(\frac{\hbar\omega}{2k_B T}\right) \tag{3}$$

$$\frac{1}{\tau_\phi} = \frac{1}{2\tau_r} + \frac{1}{2}\left(\frac{\varepsilon}{\nu}\right)^2 \lim_{\omega \to 0}\left[J(\omega) \coth\left(\frac{\hbar\omega}{2k_B T}\right)\right] \tag{4}$$
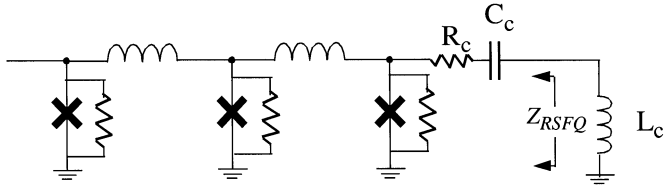
Fig. 4. The last few stages of the RSFQ Josephson transmission line which couples to the qubit. Z_{RSFQ} is the impedance of the RSFQ circuit which is used to calculate the decoherence. Linearized circuit models of the junctions are used to calculate this impedance.

τ_r and τ_ϕ are the relaxation and dephasing times, respectively. Δ and ε are the tunnel splitting and the energy bias, which relate to the energy difference ν by $\nu^2 = \Delta^2 + \varepsilon^2$. Finally, $J(\omega)$ is the spectral density due to the Johnson-Nyquist noise in the resistor, and its value can be derived from the impedance of the RSFQ circuit as shown below

$$ J(\omega) = \frac{4}{\hbar\omega} \left(\frac{M_{mw} I_p}{L_c} \right)^2 \Re\left\{ Z_t(\omega) \right\}. \tag{5} $$

Here, I_p is the qubit's persistent current, M_{mw} is the mutual inductance between the qubit and the RSFQ circuit's coupling loop, whose inductance is L_c, and $Z_t(\omega)$ is the total impedance of the RSFQ circuit in parallel with L_c. The last stage of the RSFQ circuit before it is coupled to the qubit is a Josephson transmission line, as shown in Fig. 4. Only this last stage needs to be taken into account for a sufficient approximation of the RSFQ circuit impedance. A linearized circuit model of the junction, based on the RCSJ model, was used to calculate the impedance of this stage, which, in series with the resistor and capacitor of the RLC filter, gives $Z_{\mathrm{RSFQ}}(\omega)$. The total impedance seen by the qubit is $Z_t(\omega) = Z_{\mathrm{RSFQ}}(\omega) \| j\omega L_{mw}$. This formulation gives an estimate of $\tau_r = 2.6\ \mu s$ and $\tau_\phi = 5.3\ \mu s$ as the contribution from the oscillator. Since experimental measurements on a similar qubit without the oscillator extract a decoherence time on the order of 50 ns [6], the contribution by the oscillator should be minimal.

IV. PROPOSED EXPERIMENT

The oscillator drives the qubit to rotate between $|0\rangle$ and $|1\rangle$ as shown in Fig. 3. Since the qubit also relaxes and dephases, it tends toward a 50–50 mixture of the $|0\rangle$ state and the $|1\rangle$ state if the oscillator is continuously on, and completely decays to the $|0\rangle$ state when the oscillator is turned off.

In the most recent experiments, an unshunted dc SQUID is used to detect the field of the persistent current qubit, reading out the circulating current and thus the qubit's state [8]. If the RSFQ oscillator described in this paper drives this qubit, the slow measurement process now in use cannot be synchronized with the fast rate of the RSFQ circuit. In what state such a measurement will find the qubit is a subtle question. If the qubit is undergoing continuous Rabi oscillations, then the measurement will presumably catch the qubit somewhere in its oscillations, and a single measurement will give $|0\rangle$ half the time and $|1\rangle$ the other half. Only when a large ensemble of measurements is taken will it become clear what percentage of time the qubit spends in each state. If the RSFQ oscillator is run at some duty cycle less than 50% and the relaxation time is less than 100 ns,
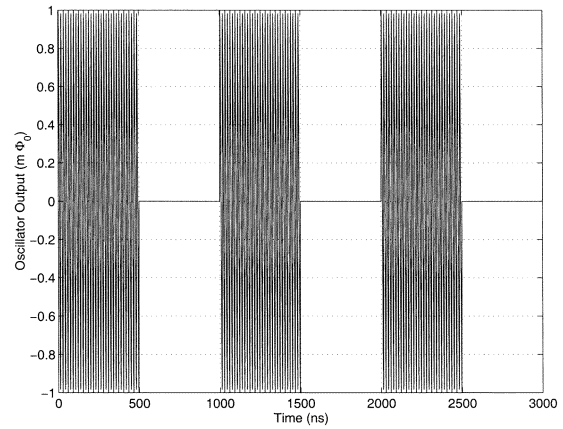
(a)
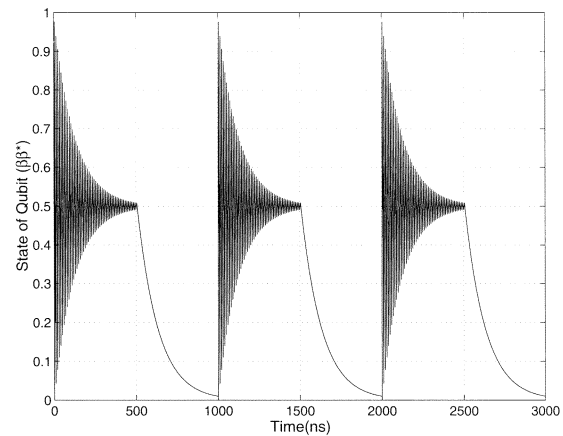
(b)
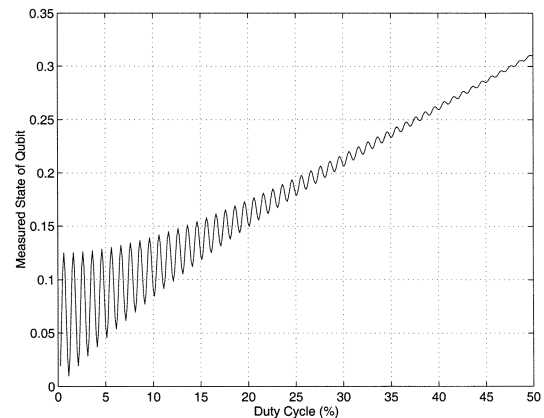
(c)

Fig. 5. (a) This is the output of the oscillator at 50% duty cycle, in units of magnetic flux seen by the qubit. The oscillations in this figure are aliased at 64 MHz in order to make the plot more readable. (b) This is the qubit response to the signal in (a). Here, the relaxation and dephasing times are both assumed to be ~ 100 ns. (c) As the duty cycle of the oscillator is varied, the mean value of the qubit response varies. The mean of (b) corresponds to 50% duty cycle, for example. If an ensemble measurement of the qubit produces the mean, then changing the duty cycle will produce the plot in (c) for the ensemble measurement. Rabi oscillations are observable in this type of measurement.

the qubit will essentially reset between pulses of the oscillator. Fig. 5(a) shows the oscillator with 50% on-time, while (b) displays the qubit response to this driving, assuming a 100 ns relaxation and dephasing time. The oscillator can be set to deliver any arbitrary rotation during its on-time, including a $\pi/2$-pulse,

a π-pulse, or a 2π pulse. In Measurement A, the qubit is rotated by a 2π pulsed, and an ensemble measurement of the qubit should produce $|0\rangle$ with just a slight perturbation should the measurement catch the qubit during its rotation. In Measurement B, the qubit is rotated by a π pulse, then the measurement should read something much closer to $|1\rangle$ than in Measurement A, even allowing for the rapid rate of relaxation to lower the probability of catching the qubit in $|1\rangle$ with the measurement. Following this reasoning gives the plot of measured qubit value versus duty cycle in Fig. 5(c). Note that the fine resolution can show Rabi oscillations in the ideal case. Even if dephasing and the slow measurement make it impossible to see the Rabi oscillations themselves, it should still be possible to get relaxation time information from this circuit.

V. CONCLUSIONS

This experiment will test the feasibility of integrating RSFQ with the persistent current qubit, and by extension, with other superconductive quantum systems. Our tests should determine the extent of difficulties caused by heating and flux noise introduced by the RSFQ circuitry. With the combination of RSFQ and quantum components, this experiment helps to develop the means to do high precision experiments on-chip, leading to integrated quantum computation circuits.

ACKNOWLEDGMENT

REFERENCES

[1] T. P. Orlando, J. E. Mooij, L. Levitov, L. Tian, C. H. van der Wal, S. Lloyd, and J. J. Mazo, "Josephson persistent-currnet qubit," *Phys. Rev. B.*, vol. 60, pp. 15 398–15 413, June 1999.

[2] Y. Nakamura, Y. A. Pushkin, and J. S. Tsai, "Coherent control of macroscopic quantum states in a single-cooper-pair box," *Nature*, vol. 398, pp. 786–788, Apr. 1999.

[3] A. Shnirman, G. Schön, and Z. Hermon, "Quantum manipulations of small josephson junctions," *Phys. Rev. Letters*, vol. 79, pp. 2371–2374, Sept. 1997.

[4] M. F. Bocko, A. M. Herr, and M. F. Feldman, "Prospects for quantum coherent computation using superconducting electronics," *IEEE Trans. Appl. Supercond.*, vol. 7, pp. 3638–3641, June 1997.

[5] J. R. Friedman, V. Patel, W. Chen, S. K. Tolpygo, and J. E. Lukens, "Quantum superposition of distinct macroscopic states," *Nature*, vol. 406, pp. 43–46, July 2000.

[6] C. H. van der Wal, J. E. Mooij, A. C. J. ter Haar, F. K. Wilhelm, R. N. Schouten, C. J. P. M. Harmans, T. P. Orlando, S. Lloyd, and J. E. Mooij, "Quantum superposition of macroscopic persistent-current states," *Science*, vol. 290, pp. 773–777, Oct. 2000.

[7] R. C. Rey-de-Castro, M. F. Bocko, A. M. Herr, C. A. Mancini, and M. J. Feldman, "Design of an rsfq control circuit to observe MQC on an rf-SQUID," *IEEE Trans. Appl. Supercond.*, vol. 11, pp. 1014–1017, March 2001.

[8] K. Segall, D. Crankshaw, D. Nakada, B. Singh, J. Lee, N. Markovic, S. Valenzuala, T. P. Orlando, M. Tinkham, and K. Berggren, "Two-state dynamics in a superconducting persistent current qubit," in ASC 2002, Houston, August 2002.

[9] K. K. Berggren, E. M. Macedo, E. M. Feld, and J. P. Sage, "Low T_c superconductive circuits fabricated on 150-mm wafers using a doubly planarized Nb/AlO$_x$/Nb process," *IEEE Trans. Appl. Supercond.*, vol. 9, pp. 3271–3274, June 1999.

[10] T. P. Orlando, L. Tian, D. S. Crankshaw, S. Lloyd, C. H. van der Wal, J. E. Mooij, and F. Wilhelm, "Engineering the quantum measurement process for the persistent current qubit," *Physica C*, vol. 368, pp. 294–299, March 2002.